Electronic Supporting Information

Oxalate-Bridging Nd^{III}-Based Arsenotungstate with Multifunctional NIR-luminescence and Magnetic Properties

Hanhan Chen, Lin Sun, Kangting Zheng, Jinpeng Zhang, Pengtao Ma,* Jingping Wang, and Jingyang Niu*

Henan Key Laboratory of Polyoxometalate Chemistry, College of Chemistry and Chemical Engineering, Henan University, Kaifeng, Henan 475004, P. R. China

Fax: +86-371-23886876; E-mail for Pengtao Ma: mpt@henu.edu.cn. and E-mail for Jingyang Niu: jyniu@henu.edu.cn.

Figures

Tables

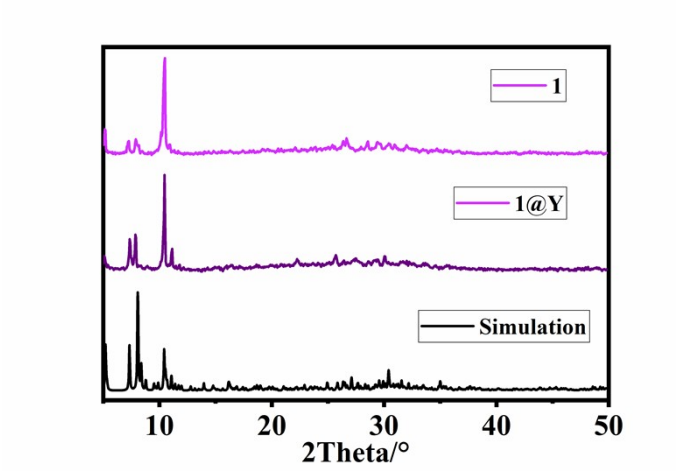

Fig. S1. The experimental and simulated PXRD patterns of **1** and **1@Y.**

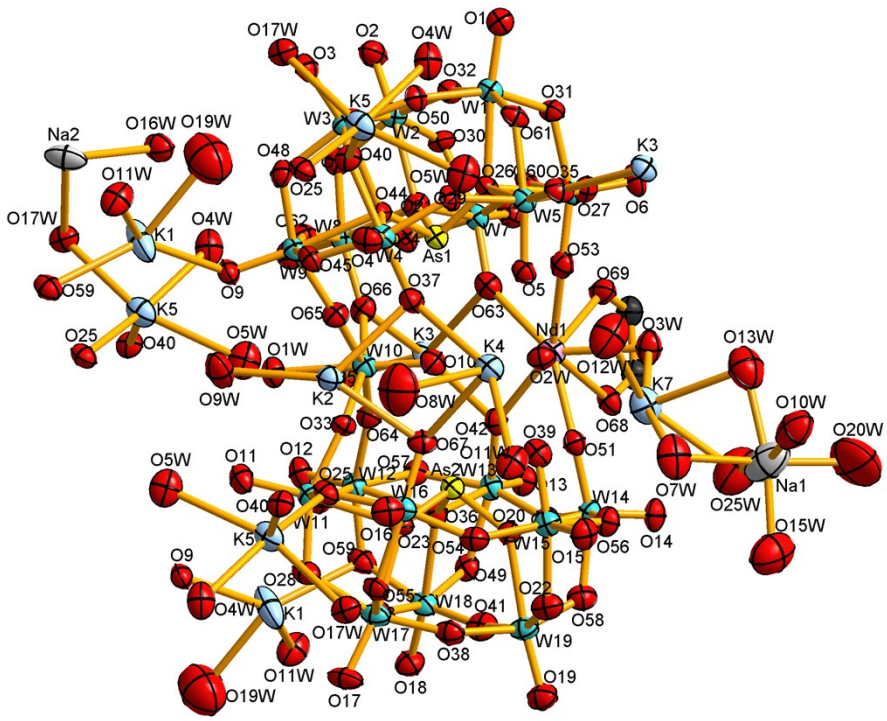

Fig. S2. Ortep diagram of the asymmetric unit in the crystal structure of **1**. All the hydrogen atoms and some lattice water molecules are omitted for clarity. (Colour code: W = aqua spheres; As = yellow spheres; Nd = lavender spheres; O = red spheres; C = dark gray spheres; K = pale bule spheres; Na = gray spheres).

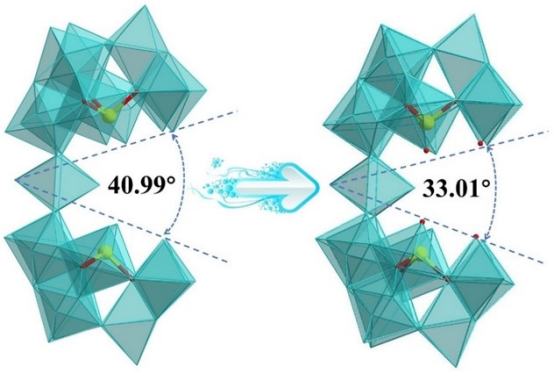

Fig. S3. The polyhedron representation of the precursor $[As_2W_{19}O_{67}(H_2O)]^{14-}$ (left); the polyhedron representation of the variable $[As_2W_{19}O_{67}(H_2O)]^{14-}$ unit in **1** (right).

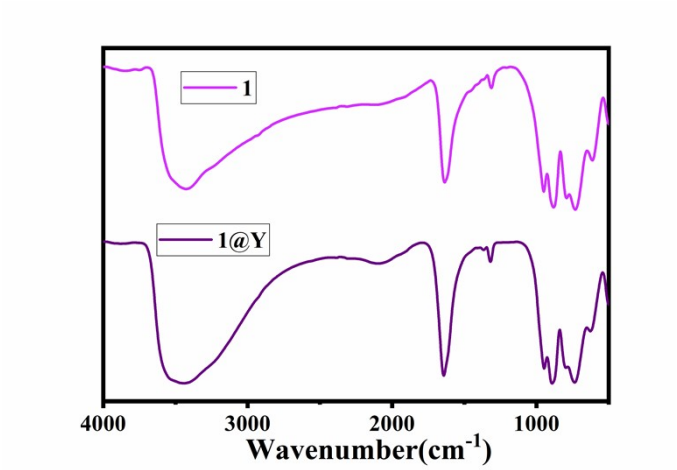

Fig. S4. IR spectra of **1** and **1@Y**.

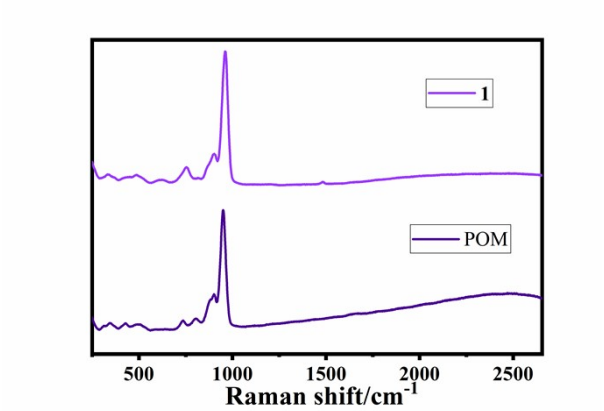

Fig. S5. Raman spectra of **1** and $K_{14}[As_2W_{19}O_{67}(H_2O)]$.

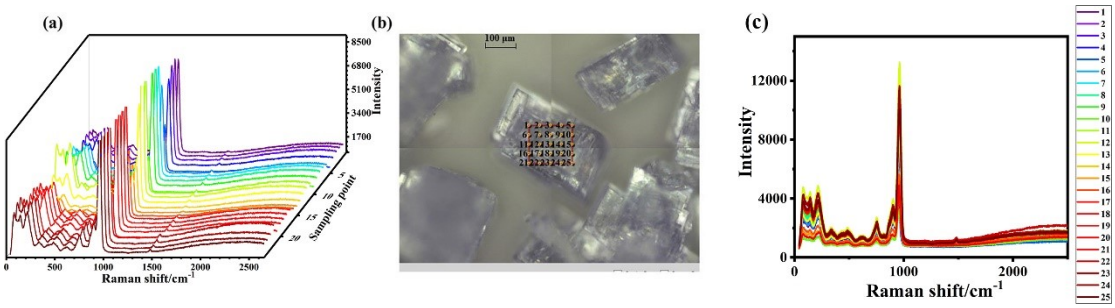

Fig. S6. (a) (c) Raman spectra at different positions on the crystal of **1**. (b) The number represent the sampling point on the crystal of **1**.

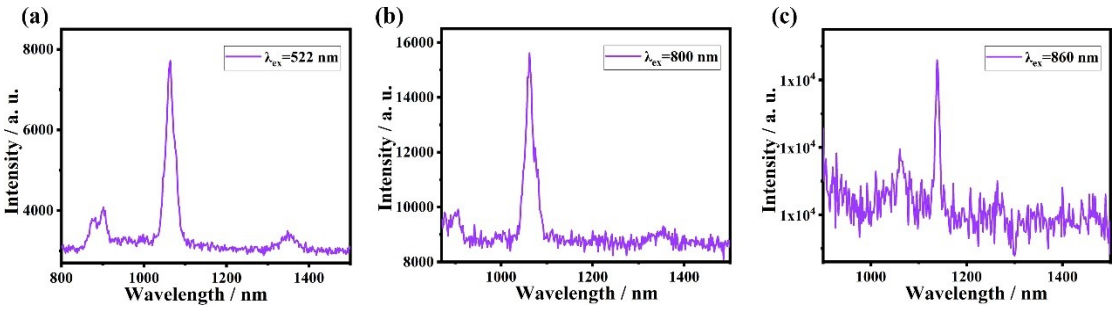

Fig. S7. The emission spectra of **1** by monitoring the excitation at 522 nm(a), 800 nm (b), and 860 nm (c), respectively.

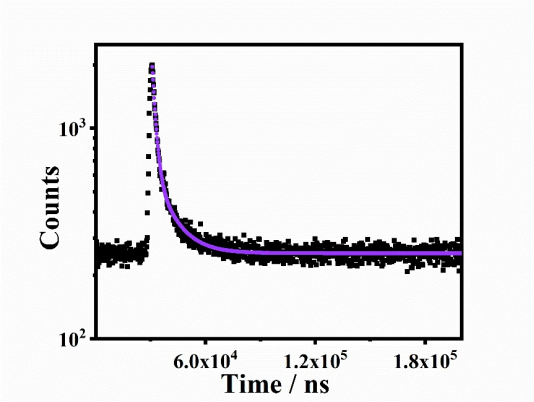

Fig. S8. The luminescence decay curve of **1** by monitoring the emission at 1059 nm upon the excitation at 580 nm.

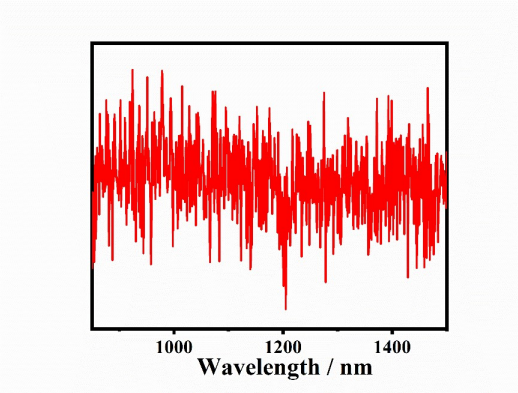

Fig. S9. The emission spectrum of $K_{14}[As_2W_{19}O_{67}(H_2O)]$ by monitoring the excitation at 580 nm.

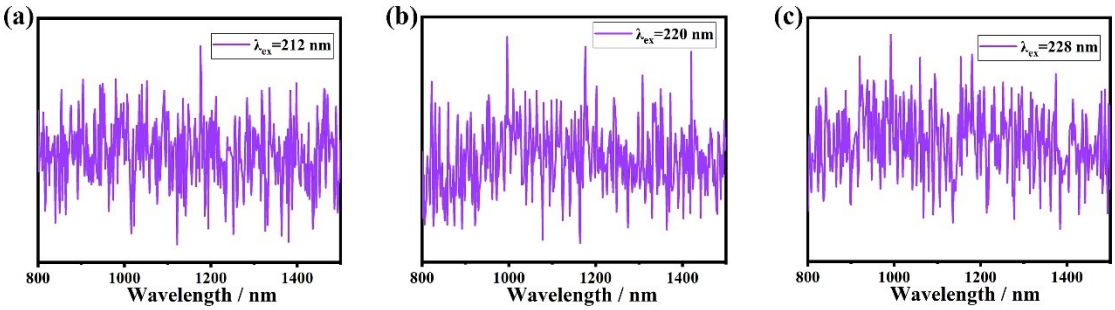

Fig. S10. The emission spectra of **1** by monitoring the excitation under 212, 220 and 228 nm, respectively.

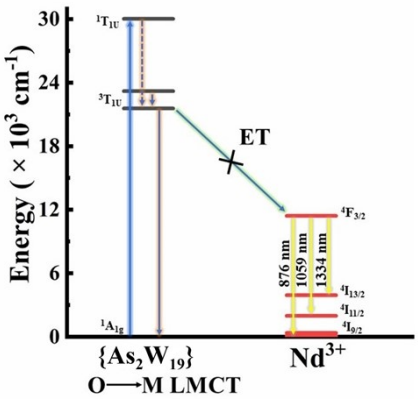

Fig. S11. The schematic energy level diagram demonstrating the mismatch of the energy gap between $^3T_{1u}\rightarrow{}^1A_{1g}$ of $\{As_2W_{19}\}$ components and $^4F_{3/2}\rightarrow{}^4I_J$ (J=13/2, 11/2, and 9/2) of Nd^{III} cations in **1**. (dotted line denotes nonradiative transition, ET: energy transfer).

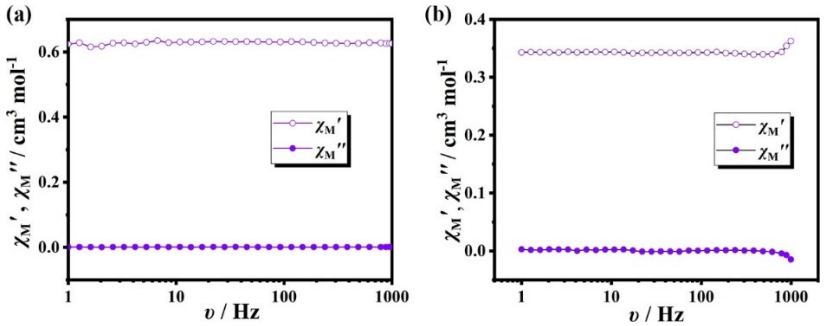

Fig. S12. Frequency dependence of χ_M' (closed circles) and χ_M'' (open circles) for **1** and **1@Y** measured under zero dc field at 2.0 K.

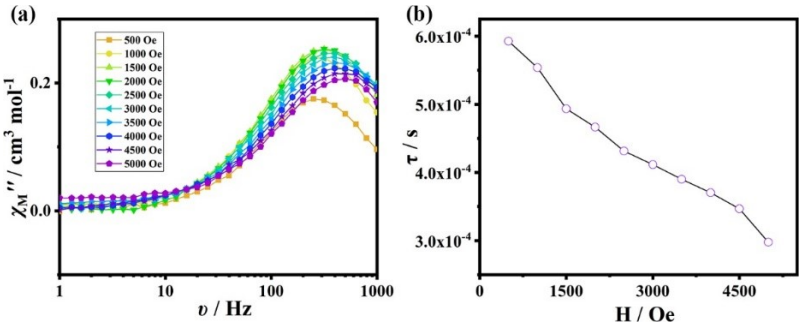

Fig. S13. Sweep field diagram of **1** from 500 to 5000 Oe, and the field-dependent relaxation time for **1** at 2.0 K.

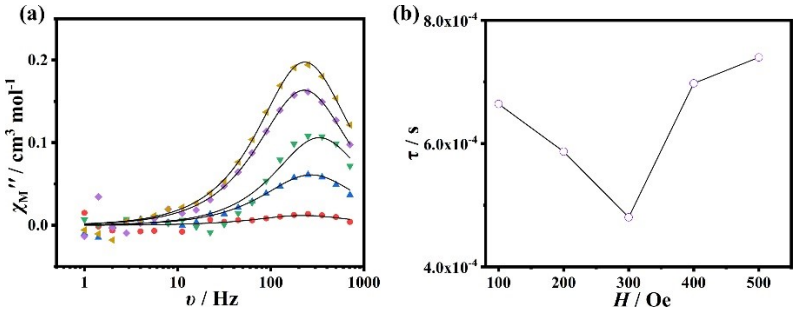

Fig. S14. Sweep field diagram of **1** from 100 to 500 Oe at 2.0 K.

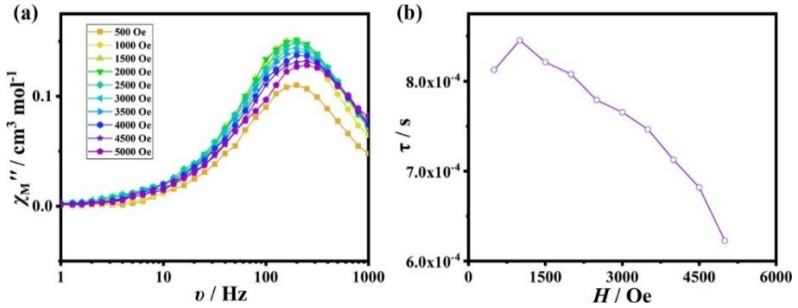

Fig. S15. Sweep field diagram of **1@Y** from 500 to 5000 Oe, and the field-dependent relaxation time for **1@Y** at 2.0 K.

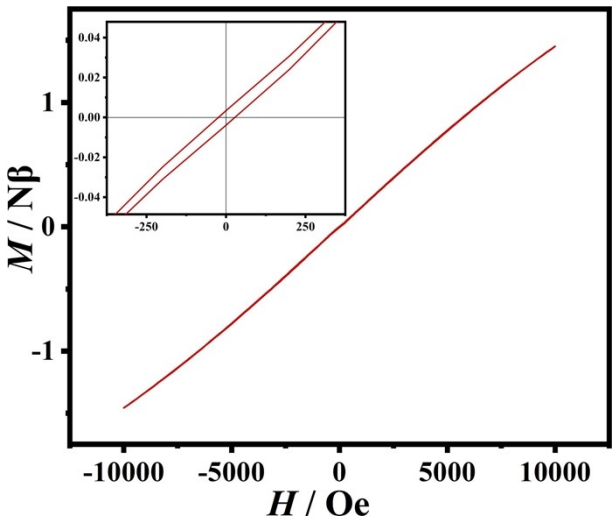

Fig. S16. Hysteresis loop for **1**, collected at 2 K with a 500 Oe s^{-1} sweep rate. Inset: expansion showing the very small coercivity (left top).

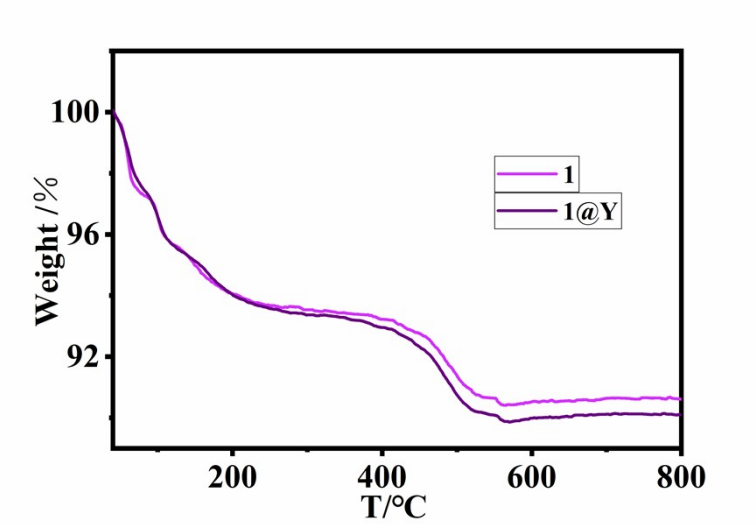

Fig. S17. TG curves of **1** and **1@Y**.

The thermal stability of **1** and **1@Y** have been determined by thermal gravimetric analysis (Fig. S17). The TG curves of **1** and **1@Y** exhibit two steps of weight loss in the range of 28–800°C. For **1**, the first stage at 28–167°C corresponds to the loss of the lattice water molecules. From 440 to 529°C, the TG trace showed a weight loss of 2.84%, corresponding to the loss of six coordinate water molecules, the dehydration of four protons, organic moieties and the decomposition of the metal-oxo cluster. For **1@Y**, the first weight loss of 6.27% from 28 to 172°C is attributed to the loss of all lattice water molecules. The second weight loss is from 439 to 510°C with a value of 3.36%, which is assigned to the six coordinate water molecules, the dehydration of four protons, accompanied with the decomposition of the polyoxoanions.

Table S1. Crystallographic data and structure refinements for **1** and **1@Y**.

	1	**1@Y**
Empirical formula	$C_2H_{140}As_4K_{14}Na_6Nd_2O_{208}W_{38}$	$C_2H_{118}As_4K_{14}Na_6NdO_{197}W_{38}Y$
Formula weight	11752.41	11498.91
Temperature / K	150	150
Crystal system	triclinic	triclinic
Space group	*P*-1	*P*-1
a [Å]	12.334(2)	12.2749(4)
b [Å]	18.595(4)	18.6068(6)
c [Å]	23.017(3)	22.8952(7)
α [°]	67.230(6)	67.2420(10)
β [°]	81.027(4)	81.1630(10)
γ [°]	79.984(6)	79.5700(10)
V [Å^3]	4770.9(14)	4722.2(3)
Z	1	1
ρ_{calcd} [g cm^{-3}]	3.911	3.840
μ [mm^{-1}]	24.449	24.725
F(000)	4904.0	4735.0
Index ranges	−14≤ h ≤ 14 −22≤ k ≤ 22 −27≤ l ≤ 25	−14≤ h ≤ 13 −22≤ k ≤ 22 −27≤ l ≤ 27
Reflections collected	59966	59535
Independent reflections	16950 [R_{int} = 0.0504]	16757 [R_{int} = 0.0556]
data/restraints/ parameters	16950/ 96/ 1154	16757/ 84/ 1068
Goodness-of-fit on F^2	1.024	1.032
R_1, wR_2 [$I > 2\sigma(I)$]	0.0442, 0.1124	0.0516, 0.1212
R_1, wR_2 [all data]	0.0530, 0.1190	0.0616, 0.1271
Largest diff. Peak/hole/e Å^{-3}	2.85/-1.92	5.27/-3.75

Table S2 BVS values for Nd, As, and W atoms in **1**.

Atoms	BVS value	Atoms	BVS value	Atoms	BVS value
Nd1	3.03	W6	5.93	W14	5.99
As1	2.92	W7	5.87	W15	5.98
As2	2.86	W8	6.04	W16	6.00
W1	6.14	W9	6.09	W17	6.04

W2	6.07	W10	6.08	W18	6.18
W3	6.09	W11	6.08	W19	6.00
W4	6.01	W12	6.23		
W5	5.91	W13	6.05		

Table S3 Possible geometries of eight coordinated metal centers.

geometry	point group	polyhedron
OP-8	D_{8h}	Octagon
HPY-8	C_{7v}	Heptagonal pyramid
HBPY-8	D_{6h}	Hexagonal bipyramid
CU-8	O_h	Cube
SAPR-8	D_{4d}	Square antiprism
TDD-8	D_{2d}	Triangular dodecahedron
JGBF-8	D_{2d}	Johnson gyrobifastigium (J26)
JETBPY-8	D_{3h}	Johnson elongated triangular bipyramid (J14)
JBTPR-8	C_{2v}	Biaugmented trigonal prism (J50)
BTPR-8	C_{2v}	Biaugmented trigonal prism
JSD-8	D_{2d}	Snub diphenoid(J84)
TT-8	T_d	Triakis tetrahedron
ETBPY-8	D_{3h}	Elongated trigonal bipyramid

Table S4 Deviation parameters calculated by SHAPE from each ideal polyhedron for Nd1.

	Nd1
OP-8	32.186
HPY-8	20.820
HBPY-8	14.644
CU-8	13.345
SAPR-8	4.852
TDD-8	3.896
JGBF-8	12.938
JETBPY-8	27.691
JBTPR-8	3.530
BTPR-8	2.664
JSD-8	5.982
TT-8	14.130
ETBPY-8	22.036

Table S5 Selected bond angles (°) of **1**.

Bond	Angle	Bond	Angle
O42-Nd1-O3W	134.9(4)	O63-Nd1-O3W	134.9(4)
O51-Nd1-O42	70.8(3)	O68-Nd1-O42	70.6(3)
O51-Nd1-O63	152.0(3)	O68-Nd1-O69	64.8(3)
O51-Nd1-O68	72.2(3)	O68-Nd1-O3W	73.4(4)
O51-Nd1-O69	131.2(3)	O69-Nd1-O42	112.7(4)
O51-Nd1-O3W	73.1(3)	O69-Nd1-O3W	73.5(4)
O53-Nd1-O42	151.4(3)	O2W-Nd1-O42	111.6(3)
O53-Nd1-O51	127.5(3)	O2W-Nd1-O51	67.0(3)
O53-Nd1-O63	70.7(3)	O2W-Nd1-O63	111.9(3)
O53-Nd1-O68	132.3(3)	O2W-Nd1-O68	134.9(3)
O53-Nd1-O69	73.5(3)	O2W-Nd1-O69	135.7(4)
O53-Nd1-O2W	66.8(3)	Nd1-O68-C1	120.4(3)
O53-Nd1-O3W	73.6(4)	Nd1-O69-C1	120.5(2)
O63-Nd1-O42	84.8(3)	O68-C1-C1	117.0(4)
O63-Nd1-O68	113.2(3)	O69-C1-C1	116.8(3)
O63-Nd1-O69	70.6(3)		

Table S6 Selected bond lengths (Å) of **1**.

Bond	Length
Nd1-O51	2.463(9)
Nd1-O42	2.490(10)
Nd1-O2W	2.460(10)
Nd1-O63	2.468(10)
Nd1-O53	2.421(10)
Nd1-O69	2.492(10)
Nd1-O3W	2.516(11)
Nd1-O68	2.500(10)
As1-O21	1.800(8)
As1-O26	1.810(9)
As1-O44	1.786(9)
As2-O20	1.812(9)
As2-O23	1.821(9)
As2-O36	1.785(10)

Table S7 Calculated and found analyses of As, W, Nd and Y with massic ratios in **1** and **1@Y**.

	sample	As (%)	W (%)	Nd (%)	Y (%)
	1	2.55	59.42	2.45	0
calcd	**1@Y**	2.61	60.73	1.25	0.77
	1	2.65	62.07	2.68	0
found	**1@Y**	2.61	62.96	1.27	0.74

Table S8 Relaxation fitting parameters from least-squares fitting of $\chi(\omega)$ data of **1**.

T / K	χ_t	χ_s	τ / s	α
1.8	1.212	0.778	7.502E-4	0.030
1.9	1.205	0.785	6.566E-4	0.022
2.0	1.206	0.794	6.015E-4	0.026
2.1	1.146	0.754	5.212E-4	0.023
2.2	1.138	0.762	4.731E-4	0.026
2.3	1.138	0.762	4.101E-4	0.051
2.4	1.125	0.775	3.937E-4	0.030
2.5	1.117	0.783	3.602E-4	0.027
2.6	1.106	0.794	3.417E-4	0.016
2.7	1.102	0.798	3.070E-4	0.019
2.8	1.094	0.806	2.866E-4	0.005
2.9	1.090	0.810	2.632E-4	0.010
3.0	1.085	0.815	2.451E-4	0.020
3.2	1.077	0.823	2.116E-4	0.027
3.4	1.067	0.833	1.841E-4	0.013

Table S9 Relaxation fitting parameters from least-squares fitting of $\chi(\omega)$ data of **1@Y**.

T / K	χ_t	χ_s	τ / s	α
1.8	1.408	0.981	0.00142	0.063
1.9	1.400	0.992	0.00124	0.059
2.0	1.374	0.993	0.00109	0.048
2.1	1.358	1.000	9.410E-4	0.060
2.2	1.344	1.001	8.265E-4	0.057
2.3	1.330	1.003	7.548E-4	0.054
2.4	1.310	1.003	6.900E-4	0.041
2.5	1.295	1.004	6.264E-4	0.029
2.6	1.282	1.005	5.724E-4	0.027
2.7	1.267	1.006	5.261E-4	0.011
2.8	1.266	1.007	4.815E-4	0.023
2.9	1.260	1.010	4.512E-4	0.020
3.0	1.254	1.011	4.260E-4	0.023
3.2	1.245	1.021	3.488E-4	0.008
3.4	1.244	1.032	3.005E-4	0.012